

Performance Investigation of Ducted Aerodynamic Propulsors

Naipei P. Bi, Kevin R. Kimmel, David J. Haas

Naval Surface Warfare Center, Carderock Division
West Bethesda, MD, USA

ABSTRACT

The aerodynamic performance of a generalized ducted propulsor system representative of those utilized for shipboard applications, which includes the shrouded duct, propulsor fan, and stators, has been investigated using a comprehensive analytical model. The model uses a panel method to represent the duct, center hub and stators, and a blade element method to represent the fan blades. Mutual aerodynamic interactions between each aerodynamic component are accounted for. Available experimental data from wind tunnel tests of comparable aerodynamic propulsors were used for validating the analytical model. Effects of aerodynamic compressibility, blockage from upstream superstructures, and various design parameters on overall performance were evaluated. Results show that compressibility effects on performance are significant when the blade tip Mach number is greater than 0.70 and can reduce the efficiency of the ducted fan system by more than 10% depending on the airfoils used, blade pitch setting, and specific operating condition. Inlet flow blockage from superstructures upstream of the ducted propulsor system was also simulated. Results indicate that significant vibratory loads are induced in both the rotating and fixed frames when a quarter of the duct inlet is blocked. A thorough evaluation of the blockage effects should be conducted if a ducted propulsor is used on surface ships where significant superstructures exist upstream of the ducted propulsor. Effects on performance due to other design parameters such as blade tip clearance, blade twist, and the relative location of the fan within the duct were also evaluated.

Keywords

Ducted, propulsor, aerodynamics, compressibility, blockage.

1 INTRODUCTION

High performance ducted aerodynamic propulsors are a critical component of future Naval amphibious surface ship planforms such as next generation Landing Craft Air Cushion (LCAC) vehicles, Surface-Effect Ship (SES) concepts, and Sea-Base-Connector Transformable Craft (T-Craft). In order to achieve an optimal propulsor design,

a comprehensive analytical tool is required to accurately and efficiently analyze the aerodynamic performance of an entire ducted propulsor system which includes the shrouded duct, fan, center hub, and rudders as well as pre-swirl and/or post-swirl stators. Unlike hydrodynamic ducted propulsors used in water, a ducted aerodynamic propulsor system used above the water line can possess strong compressibility effects due to requirements for blade tip speed to be in the moderate to high subsonic speed range. Also, mutual aerodynamic interactions among different components, i.e., fan, duct, stators, rudders and upstream superstructures can be severe. The non-uniform inflow induced by the superstructure upstream of the ducted propulsor and the wave fence along the outboard side of the duct can have a significant impact on performance, which further complicates the analysis and optimization of a ducted propulsor system.

Ducted propulsors of various designs have been used for many years and a substantial amount of research has been focused in the past on both aviation and marine applications. In hydrodynamics application, for example, among others (Black, 1967, 1968; Morgan 1968, and Worobel, 1968), Morgan made a summary of the comparison of theory and experiment on ducted propellers in 1968 and concluded that in general, the available theories could give an adequate prediction of the forces and pressure distribution if no separation occurs on the annular airfoil and, in addition for ducted propellers, if a sufficient mathematical model of the propeller is used. For aviation applications of ducted fans, many researchers have studied performance in various flight environments (He, 2006; Marc, 2001; and Bi, 2008). With increasing demands in designing the next generation water surface crafts/ships such as the replacement of the LCAC, as well as SES and the T-Craft concepts, growing interest has been generated in having a comprehensive analytical model that can be used to analyze and optimize the complicated aerodynamic performance of future ducted propulsors accurately and efficiently.

To understand the complete aerodynamic flow field associated with a ducted propulsor, a Computational Fluid Dynamics (CFD) approach, which is very powerful, can be adopted. However, using a CFD approach to investigate various aerodynamic interactions for different configurations over a broad range of operating conditions

becomes impractical due to the enormous computational time required. Conversely, analytical codes currently available for ducted aerodynamic propulsor preliminary design are not computationally demanding, but are typically based on the lifting line theory and/or empirical data, which limits their usefulness in accounting for complicated aerodynamic phenomenon such as compressibility effects due to high fan tip speeds, and blockage effects due to superstructures located upstream of the propulsor. Therefore, an alternate analysis approach which can accurately and efficiently support the design and analysis process of a complete ducted propulsor system is needed. The objective of this study is to develop and refine an analytical model that can provide both accurate and efficient calculations of performance, including significant aerodynamic interactions, and therefore, support the design and optimization process of a complete ducted aerodynamic propulsor system. The technical approach is to use a blade element method to represent the propulsor blades and a panel method for the shrouded duct, center hub and stators. With this approach, mutual aerodynamic interactions between the fan blades, shrouded duct, and other aerodynamic components such as stators and center hub can be directly accounted for. Aerodynamic compressibility effects on performance can also be accounted for through the incorporation of 2-D airfoil nonlinear aerodynamic characteristics in tabular form. A generalized representation of blockage effects from superstructures upstream of the ducted propulsor and the wave fence along the outboard side of the propulsor duct is also included by using a non-uniform free stream. With this model the effects of various important design parameters such as blade twist distribution, the clearance between the blade tip and the shrouded duct, and solidity can also be evaluated.

2 ANALYTICAL MODELING

2.1 Analytical approach

An effort has been made to build a robust analytical model to analyze the steady and unsteady aerodynamic performance of a ducted aerodynamic propulsor. In this effort, the propeller was modeled using a blade element method while the duct, hub (center-body), and stators are modeled using the panel method. Due to the complexity of the aerodynamic environment, there are strong aerodynamic interactions between each component of the ducted propulsor. The superstructure located upstream of the ducted propulsor is another strong source of aerodynamic interferences because not only is it usually located very close to the duct inlet, but it also creates strong non-uniform inflow to both the duct and propeller. In this analysis, the interference of the duct, stators and center hub on the propeller is considered in two parts. The first is the interference of the panel duct, stator and center-body on the propulsor blade surfaces, which is computed

at each aerodynamic computational point (ACP) of the fan blade element segments. The second is the effect of the blades on the duct, stators and center hub, which is considered using an enhanced finite state dynamic fan wake model (He, 2006). The fan induced velocities on the duct, stators and center hub are computed at each panel ACP including the induced velocity components in all three axes. All features are implemented within the comprehensive rotorcraft analysis software, FLIGHTLAB (ART, 2004).

Because a combination of the panel method for the duct, stators, and center hub, and blade element method for the blade is used and all aerodynamic interactions are considered, this model can be used to analyze the performance of a generalized ducted aerodynamic propulsor accurately and efficiently. This analytical model can also be used to conduct sensitivity studies of various design parameters such as blade planform, clearance between the blade tip and shroud, and the relative location (i.e., depth) of the fan within the surrounding duct. In addition, the model can be used to study aerodynamic compressibility effects and to analyze the blockage effects due to the presence of superstructure upstream of the duct.

2.2 Validation of the analytical model

Validation of the analytical approach was conducted with available experimental data collected in wind tunnel tests of two different ducted fan systems evaluated at approximately 1/6 scale in two different 8' by 10' subsonic wind tunnels. The first ducted fan system was an aviation related "fan-in-disk" configuration which consisted of a circular duct, center cabin, fan and stators. Correlation between analytical model and wind tunnel test data was performed over a range of fan rotational speeds in hover conditions. Prediction accuracy of the current analytical model is within 5% for thrust and within 7% for torque for the range of fan rotational speeds (Bi, 2008). The second set of experimental data available was a shrouded fan system designed as an aerodynamic propulsor for a future ship concept. This system has a duct, fan and stators. Good agreement was also achieved in both total thrust and the shaft power (i.e., within 7% in thrust and 10% in power). Qualitative trends for thrust and torque as a function of fan rpm and advance ratios were also similar. Due to the proprietary nature of the ducted propulsor model, no results have been published in the public domain. Both of these ducted fan wind tunnel test data sets included a broad range of fan rpm and advance ratios. The relatively good agreement with this limited available experimental data provided the authors with a degree of confidence that the analytical model accurately captured the overall flow field of the ducted fan system and as such could be utilized to study the performance characteristics of a generalized ducted propulsor system.

2.3 Description of baseline configuration

A baseline configuration that represents a generalized ducted aerodynamic propulsor system representative of typical shipboard applications including fan, stators and a center hub is used in this study. Table 1 lists characteristic parameters used for the baseline configuration. Selection of the design parameters shown in Table 1 was mainly based on the statistics collected from reports on various ducted aerodynamic propulsors for shipboard application. The duct diameter is constrained by the space available on the craft that normally requires having a wide enough space between ducted propulsors for loading and unloading military vehicles and equipment. The duct is assumed to have a constant diameter along the axial direction. Theoretically, it is better to have a duct that has a few degrees of divergence in the duct axial direction to compensate for the accumulation of the boundary layer growth along the duct inner wall, although this effect is not considered in this study. For hydrodynamic applications, it is known that a decelerating ducted propeller is often required for reducing the risk of propeller blade cavitations when it operates in the water. However, for ducted aerodynamic propulsors, fan blade cavitation is not a concern.

Table 1: Baseline configuration characteristics

Propulsor diameter, d	12 ft
Duct length, l	6 ft
Number of blades	6
Nominal propeller rotational speed, n	1300 rpm
Blade tip Mach number	0.73
Blade nonlinear twist	40 deg
Solidity	0.45
Blade tip clearance	1% Radius
Number of stators	7
Blade airfoil	NACA 0012

Figure 1 shows the panel model for the duct, stators, and center hub of the baseline configuration. The classical NACA 0012 airfoil is used for the fan blades because its aerodynamic characteristic data are readily available. Although the NACA 0012 airfoil is not an optimum choice for achieving the most efficient ducted propulsor, it can be a useful baseline for comparison purposes. This choice does not affect the goal of the present study in so much as the objective is to investigate the basic aerodynamic performance of a ducted propulsor and the

relative changes in performance by varying design parameters. Variations include twist angle, blade tip clearance and the relative location of the fan within the duct. Also, compressibility effects were investigated using the baseline configuration and another configuration with advanced airfoils.

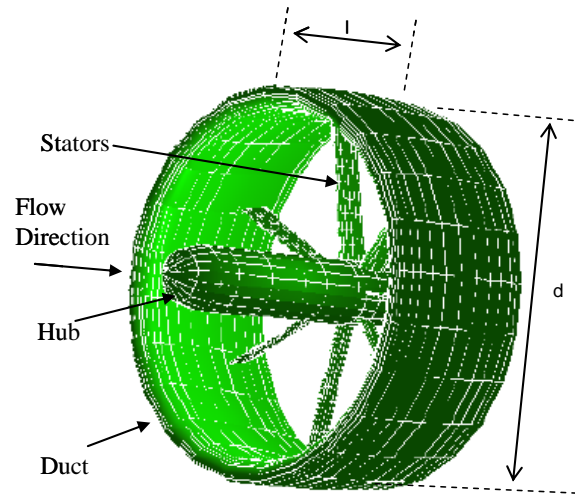


Figure 1: Panel model of duct, stators and center hub (fan blades not shown)

3 RESULTS AND DISCUSSION

An initial performance assessment of the baseline configuration was conducted. Compressibility effects were investigated in both the static (bollard) condition and at various advance ratios or craft speeds. Following this, a simulation of the superstructures located upstream of the duct inlet was done by blocking a quarter of the fan disk from free stream flow. In addition, the effects of variations in several design parameters on performance were evaluated as well.

3.1 Performance of baseline configuration

Performance of the baseline configuration in the bollard condition was examined first. It is known that in the static (bollard) condition, the rotating fan within the duct will generate considerable suction around its inlet such that additional thrust will be generated by the duct. Based on momentum theory, the duct could generate as much thrust as the fan in the static condition. The duct thrust generated depends on the ratio of velocity at the fan disk to wake velocity downstream. When this ratio is one (i.e., the duct has kept the slipstream downstream of the fan disk from contracting), the duct thrust is equal to the fan thrust. Practically, it is very challenging for the duct to generate the same amount of thrust as the propulsor due to various reasons such as imperfect duct section shape, flow distortion around the duct inlet, adverse aerodynamic interactions between the duct and other aerodynamic and structural components, and flow separation inside the duct. Figure 2 presents the duct contribution to the total thrust

for the baseline configuration in the bollard condition. The blade rotational speed is 1,300 rpm. It can be seen that overall, the duct contributes approximately 35% - 42% of the total thrust over a range of pitch angles. Even though the duct contribution to the total thrust is approaching the ideal limit of 50% of the total thrust, it is believed that these magnitudes are realistic based on wind tunnel test results.

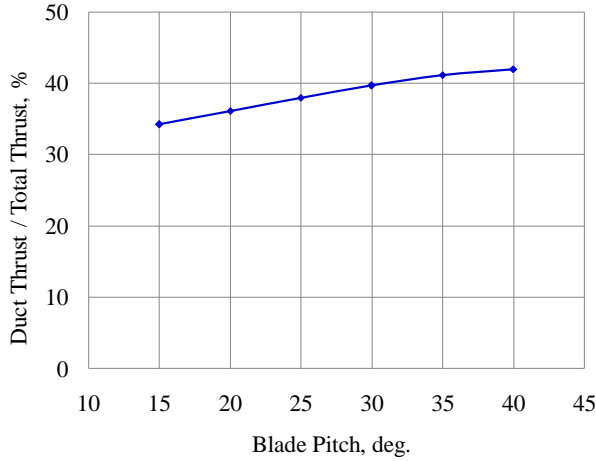


Figure 2: Duct contribution to total thrust in bollard condition

Figure 3 shows the total thrust, and the contributions to the total thrust by the fan and the duct over a range of free stream speed. The propulsor pitch angle, θ , is 30 deg and the fan rotational speed is 1,300 rpm. The Y-axis of Fig. 3 is the thrust normalized by the total thrust in the bollard condition. It can be seen that the total thrust decreases with increasing free stream speed and the reduction in total thrust is due to a loss in both the propulsor thrust and the duct thrust. If aerodynamic interactions are ignored, the reduction in propulsor thrust can be explained as follows: as the free stream speed increases, the induced angle increases for a fixed pitch angle blade, which results in a decrease in the effective angle of attack along the blade and therefore, a reduction in fan thrust as long as the effective angle of attack is below the stall angle.

The results in Fig. 3 also indicate that the duct thrust drops much faster than the fan thrust for the baseline configuration. One way to understand this effect is to consider an open fan (no duct) at high forward speed. In this operating condition, the free stream convects the fan wake rapidly downstream resulting in little or no effective wake contraction. Adding a duct around this uncontracted wake does not change the wake contraction and, therefore, from momentum theory, does not result in the generation of thrust. In addition, the duct can have a significant drag if the free stream speed reaches high subsonic speed, due to possible shock waves on the duct surface. However, at the relatively low operating speed range for surface ships (i.e., below 50 kts, which is less than a Mach number of 0.1), the duct can still make a significant contribution to the total thrust. Figure 3 shows that at 50 kts, the duct

generates approximately 25% of the total thrust for the baseline configuration. Therefore, it is very important to maximize the duct contribution to the total thrust for a ducted aerodynamic propulsor for shipboard application.

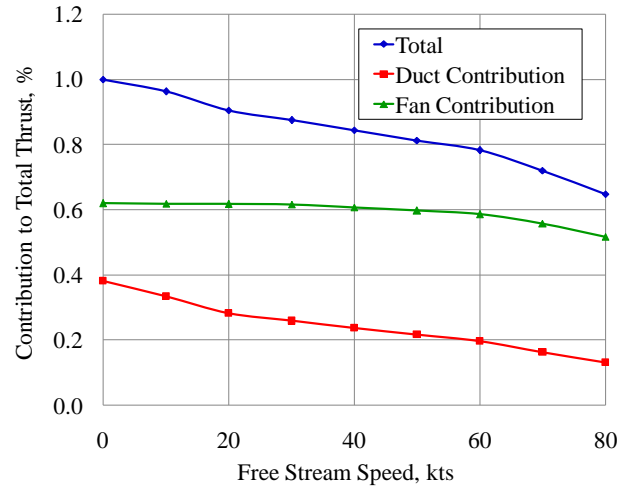


Figure 3: Variation in duct thrust with increasing free stream velocity

As for an open propeller, propulsor efficiency (η) can be used as a measure of the performance of a ducted aerodynamic propulsor system, where η is defined as:

$$\eta = J/2\pi K_t/K_q \quad (1)$$

where J is the advance ratio, $= V/(n \cdot 2 \cdot R)$. V is free stream or craft velocity in ft/s, n is the propulsor rotational speed in revolutions per second (rps) and R is the propulsor radius in ft. The parameter K_t is defined as total thrust divided by $(\rho \cdot n^2 \cdot (2 \cdot R)^4)$ where ρ is the air density, and the parameter K_q is defined as the total torque divided by $(\rho \cdot n^2 \cdot (2 \cdot R)^5)$. The efficiency of the baseline configuration at three different pitch angles and a blade rotational speed of 1,300 rpm is shown by Fig. 4. The maximum advance ratio examined is 0.515 which corresponds to a free stream velocity of 80 kts (beyond the normal range of surface ship speeds). At a low pitch angle of 15 deg, the baseline configuration reaches a maximum efficiency of approximately 0.62 at an advance ratio of about 0.40 where the operating velocity is approximately 60 kts. As the pitch angle increases, the efficiency decreases at low advance ratios where the ducted propulsor is normally designed to operate. Figure 4 indicates that to have a greater efficiency, the blade pitch setting should be 15 deg for this baseline configuration. However, in reality, it might not be possible to use this pitch setting because the requirement for maximum thrust is greater than the amount produced at 15 deg. Higher thrust levels can be achieved by increasing the blade pitch setting or fan rpm. However, maximum pitch angle is limited by blade stall angle over which lower fan blade section lift will be accompanied by higher drag. Higher fan rotational speed results in higher fan blade tip speed, therefore, there is a higher possibility of having

undesirable aerodynamic compressibility effects (i.e., greater drag). Compressibility effects on performance will be discussed in the following section. In practice, it is necessary to study the effects of various design parameters such as solidity, number of blades, blade twist and taper ratio on performance in order to achieve high efficiency in the desired operating range.

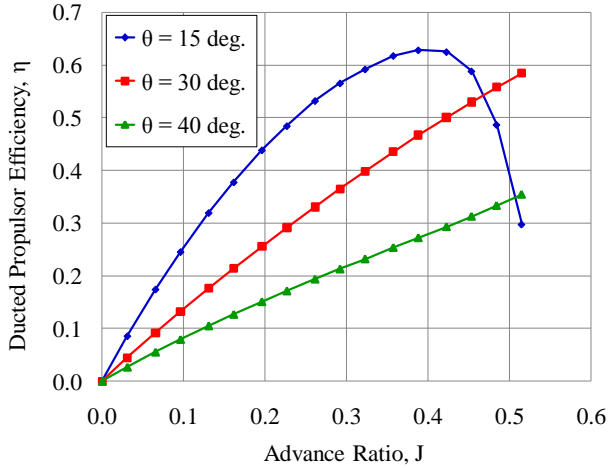


Figure 4: Ducted propulsor efficiency at various advance ratios

3.2 Compressibility effects

Mach number (ratio of the flow speed to the speed of sound) can be understood as a ratio of inertia forces in the flow to the forces resulting from compressibility and is used to characterize the degree of compressibility. When air flows past an airfoil, the local velocity at the surface outside the boundary layer may be greater or less than the free stream velocity. The highest velocities occur near the leading edge and over the upper surface of the airfoil and can become transonic (i.e. Mach number near one) depending on the pitch angle and free stream speed. Usually, higher pitch angles result in higher Mach numbers on the upper surface of the airfoil. For high subsonic or transonic flow, the aerodynamic characteristics of an airfoil can be very different from the incompressible flow condition (i.e., at low Mach numbers). This can result in a severe adverse effect such as very low ratio of lift to drag and even local shock waves on the surface of the airfoil.

Like the open propulsor, the blade tip speed or tip Mach number of a ducted aerodynamic propulsor should be kept low enough such that the adverse effect of aerodynamic compressibility does not significantly reduce overall performance or efficiency. In practice, due to the constraint on the size of the duct (or propulsor diameter) and the requirement for sufficient thrust to propel the craft beyond the designed “hump speed” with gusts, the propulsor needs to run at a relatively high tip speed. Normally, the blade tip speed is selected anywhere from 750 to 850 ft/s. At sea level on a standard day, the speed

of sound is approximately 1,116 ft/s. Therefore, the corresponding Mach number of the flow before reaching the leading edge of the blade tip can be anywhere from 0.66 to 0.76. Hence, the local Mach number on the upper surface of the blade tip region can be greater than 0.80 or can even reach 1.0 depending on the pitch angle. In this case, the compressibility effect on performance is very significant and should be investigated during the blade design including the airfoil selection process.

For the purpose of studying the compressibility effect on the performance of a ducted aerodynamic propulsor, a second configuration was developed and denoted as the “incompressible flow configuration”, in which no compressibility effect is included in the 2-D airfoil aerodynamic characteristics tables. For this configuration, airfoil aerodynamic characteristics at different Mach numbers are set equal to that at zero Mach number (i.e., incompressible flow). Although, this configuration does not simulate reality it provides a useful means to characterize the compressibility effects on performance. To compare the efficiency in the static (bollard) condition between the baseline configuration and the incompressible configuration, a parameter called power loading (PL) is used. PL is defined as the ratio of the total thrust, T_{total} , generated by the entire ducted aerodynamic propulsor system to the corresponding fan shaft power required:

$$PL = T_{total} / \text{Power, lbs/hp} \quad (2)$$

As expected, the efficiency is decreased as the blade tip Mach number increases. Figure 5 shows the reduction in efficiency (PL) due to the compressibility effects in the bollard condition at two different blade pitch settings (25 and 30 deg) with different blade rotational speeds, i.e., different blade tip Mach numbers. The Y-axis represents a ratio of the PL with compressibility effects to the PL without compressibility effects. It is clear from Fig. 5 that for the baseline configuration with the NACA 0012 airfoil, as Mach number increases, the efficiency degrades quickly. When the blade tip Mach number reaches 0.68, the efficiencies are reduced by approximately 14% for a pitch angle of 30 deg and by 6% for a pitch setting of 25 deg. The efficiencies are further reduced by approximately 19% and 10% respectively when the fan tip Mach number reaches 0.73.

Similar compressibility effects on the efficiency at different advance ratios are shown by Fig. 6 where the blade rotational speed is 1,300 rpm. At $J = 0.30$, which is equivalent to a speed of 46 Kts, the efficiency is reduced by approximately 14% for a pitch setting of 30 deg and 5% for a pitch setting of 25 deg, which is again very significant. Therefore, the compressibility effect has to be considered in the ducted aerodynamic propulsor design. It can be less or more severe than that shown by Fig. 6 depending on the local effective angle of attack at each propulsor blade section.

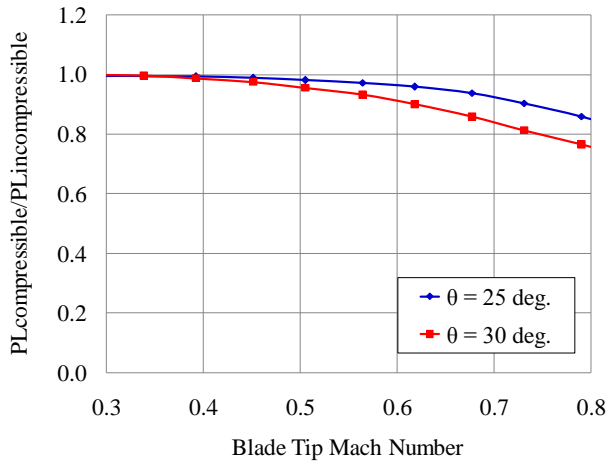


Figure 5: Effect of compressibility on efficiency versus tip Mach number (NACA 0012)

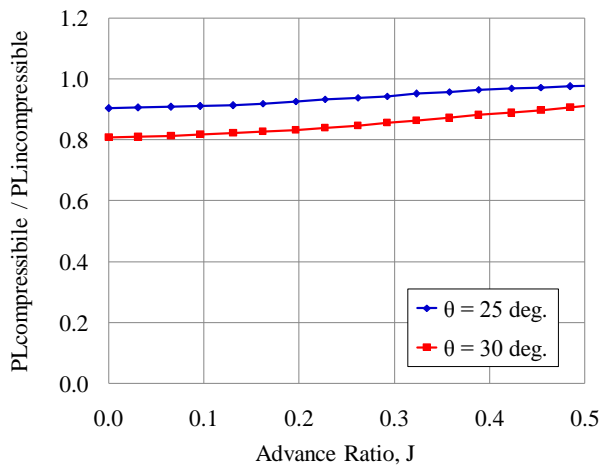


Figure 6: Effect of compressibility on efficiency versus advance ratio (NACA 0012)

To understand the physics of the reduction in efficiency at high subsonic Mach number, it is necessary to understand the aerodynamic characteristics of the airfoil used. Essentially, to achieve a highly efficient blade requires that each section of blade should operate at a high ratio of lift to drag, L/D . Therefore, the performance of L/D for a given airfoil within a blade is an indication of what the performance of this blade can be. Figure 7 shows the L/D of a NACA 0012 airfoil for several Mach numbers. One basic aerodynamic characteristic in Fig. 7 should be noted. This is the change in maximum L/D with Mach number. In general, as the Mach number increases, the maximum L/D decreases. For the NACA 0012 airfoil, the maximum L/D decreases from 63 at $M=0.4$ to 55 at $M=0.6$ and further to 45 at $M = 0.7$, which corresponds to reduction by 13% and 29%, respectively. A larger drop in L/D occurs at $M = 0.80$ where the reduction is by 67% from that at $M = 0.4$. This large decline in L/D at high Mach numbers will definitely degrade the overall performance of a ducted aerodynamic propulsor. Proper measures should be taken to alleviate the compressibility effect and further discussion is given in following sections.

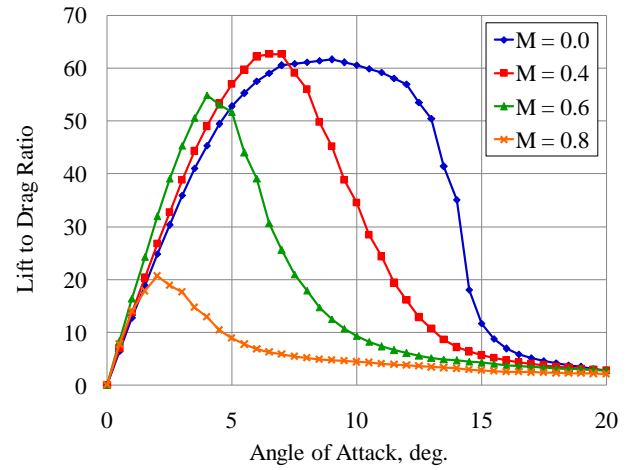


Figure 7: Lift to drag ratio of NACA 0012 airfoil

The selection of airfoil shape plays a very important role in determining the compressibility effects. Instead of using NACA 0012 airfoils, an airfoil series called RC airfoils (developed by NASA Langley Research Center for rotorcraft applications) were used in the current study to evaluate the compressibility effects. The RC(4) airfoil is used for the inner portion of blade and the RC(3) airfoil is used for the outer portion of blade (Bingham, 1982). Figure 8 shows the maximum L/D for the RC 310 airfoil. To make a comparison with a NACA 0012 airfoil, the maximum L/D of the NACA 0012 is also plotted in Fig. 8. Two distinctions are observed from this comparison: (1) the RC 310 airfoil has a much larger maximum L/D and (2) between the Mach numbers of 0.4 and 0.6, instead of a gradually decreasing maximum L/D as shown by the NACA 0012 airfoil, the maximum L/D for the RC 310 airfoil is actually larger than those at Mach numbers less than 0.4, which is helpful in alleviating the compressibility effects in this range of Mach numbers.

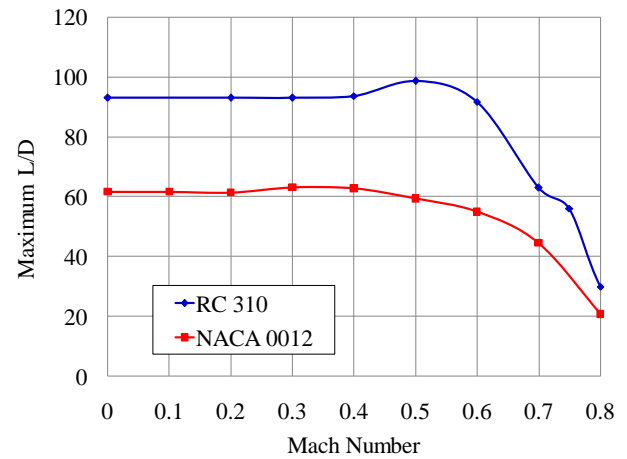


Figure 8: Maximum L/D comparison between NACA 0012 and RC 310 airfoils

Figure 9 shows the compressibility effects on the PL in the static condition for the blade with RC airfoils and the blade with the NACA 0012 airfoil for comparison. When Mach number is less than 0.5, compressibility has little

effect on the RC airfoils. As the Mach number further increases, compressibility starts to show its impact and the efficiency decreases. For example, when the blade tip Mach number reaches 0.73 the efficiency has been reduced by 10%, which is much less severe when comparing to the NACA 0012 airfoil, but still very significant. From Fig. 9, it can also be seen that using advanced airfoils can minimize the compressibility effect in a certain range of Mach numbers. However, the adverse effects of aerodynamic compressibility on performance cannot be totally eliminated when blade tip speed is in the high subsonic or transonic speed range. In addition to airfoil choice, another way to lessen compressibility effects is to use a properly tapered and/or swept blade tip.

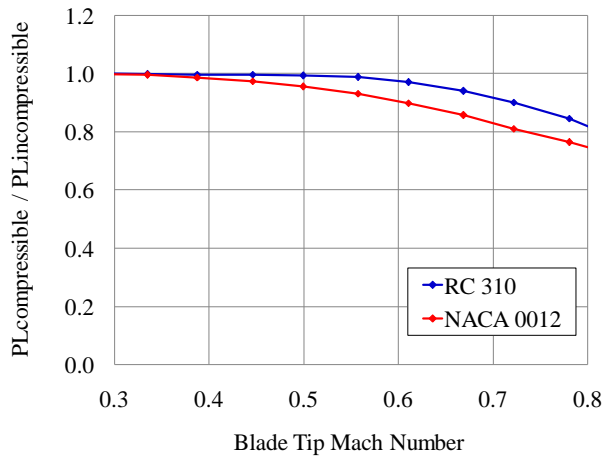


Figure 9: Comparison of effect of compressibility on efficiency between NACA 0012 and RC airfoils

3.3 Blockage effects

For amphibious surface ship planform applications, there is usually some type of superstructure located in front of a ducted aerodynamic propulsor system. Depending on the size, shape and the proximity to the duct inlet, the superstructure can create a complex flow field including blockage of air flow, swirl flow, and flow separation behind the superstructures, which has a direct effect on the quality of the flow into the ducted propulsor system. Also, to shield the propulsor from waves along the side of the ducted propulsor system, a side panel or wave fence is usually installed, which will create additional blockage to the flow that goes into the duct. The net effect due to superstructure and wave fences is that the air flow into the duct is no longer uniform either in direction or in magnitude. For example, a detailed flow survey was conducted (Gowing 2003) at various radial and angular locations centered on the propeller shaft for two stations upstream of the duct behind the superstructure of a full scale Landing Craft Air Cushion (LCAC) vehicle. Test conditions included multiple speeds over water as well as bollard conditions at full power. It was concluded that severe velocity deficits were found in the lower outboard

quadrant of the inflow, and these deficits became more severe closer to the back face of the craft superstructure.

In reality, if the superstructures are box-like and have sharp corners, the pressures behind the superstructures can be very low (like a vacuum) such that a re-circulation flow region can be formed just behind the superstructure. In the worst case scenario, due to the high negative pressure behind the superstructure, the flow downstream of the propulsor may even flow back around the outside of the duct to the front of the duct to form another re-circulation zone, which can make the flow condition more complicated. This complex non-uniform flow field can impact not only the overall performance but also the vibratory loads in both the rotating frame and fixed frame of a ducted aerodynamic propulsor system. In the rotating frame, significant oscillating normal shears (out of plane forces) at the blade root will affect the blade fatigue life, and therefore should be considered in the blade design. In the fixed frame, the vibratory loads should also be considered as they will be directly transmitted through the propulsor attachment into the hull.

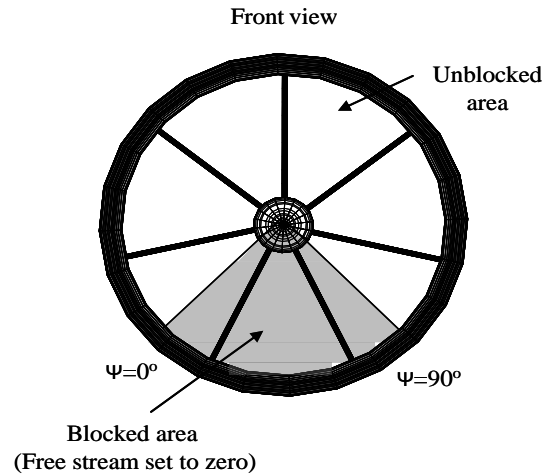


Figure 10: Propulsor inlet blockage area

In the current analysis, the total axial flow experienced by each aerodynamic component such as propulsor blade and duct is the sum of three axial flow components; fan self induced inflow, interference from other aerodynamic components (mutual aerodynamic interactions) and the free stream flow (craft speed or gusts). Fully simulating the impact of superstructures and wave fences is very challenging because of the complicated nature of the interactions and varies according to specific design features. In order to evaluate the effects of blockage in a generalized sense, a model that simulates the blockage effect on the free stream flow in the axial direction over a partial space of the duct inlet has been developed. Figure 10 illustrates the blockage area used in this study. In Fig. 10, ψ is the blade azimuth angle. Preliminary results are obtained with a generalized representation of blockage in which a quarter of the fan area is fully blocked from the free stream to represent a typical shipboard propulsor installation. The blockage region experiences zero free

stream velocity and the flow only consists of self induced and mutual aerodynamic interactions.

Figure 11 shows the relative fluctuation of the blade root normal shear force (out of rotational plane) during one blade revolution (azimuth from zero to 360 degrees) at a free stream speed of 30 kts. The Y-axis in Fig. 11 represents the normal force at the blade root (total thrust generated by a blade) normalized by the averaged force along a full cycle. Without any blockage, all values should be one. However, with blockage it is observed that in the blocked region (azimuth from zero to 90 deg), blade normal force is increased. The level of local thrust increase is seen to be dependent on the pitch angle settings. This increase in thrust is due to the decrease in the free stream velocity (i.e., the increase in the effective angle of attack because the blade pitch and rotational speed are held constant). This observation is correct as long as the stall angle is not reached. If the blade is operating near but not above the stall angle, the overall blockage effects on blade thrust can be different because blockage effects may push the effective angle of attack over the stall angle. Correspondingly, blade lift can be increased or reduced depending on the proximity of the effective angle of attack with respect to the stall angle. If the effective angle of attack is above the stall angle, the drag experienced by a blade will increase and more power will be required for the same amount of thrust created at an effective angle of attack lower than stall angle. Another phenomenon observed is that the blockage can cause the lifting distribution over a full rotation cycle to vary nonlinearly. This is because of the mutual aerodynamic interactions among each section of blade and between blades and duct. The third phenomenon observed is that a larger relative increment in thrust occurs at lower blade pitches. Further, it is observed that as the pitch increases, the relative change in thrust during each revolution decreases. This is because at a larger pitch setting, the angle of attack is larger and therefore, blade induced inflow accounts for a higher portion of the overall inflow. Consequently, the free stream contributes proportionally less to the total inflow and hence, plays a smaller role in the blockage effect.

In an axially symmetric flow environment, the ducted propulsor should generate steady, uniform thrust and torque. However, when there is a blockage over part of the ducted propulsor, oscillating forces and moments acting on each blade in the rotating frame will be transmitted to the hub (fixed frame) in the form of 6/rev forces and moments for a six-bladed propulsor. Also, the non-rotating parts such as duct, stators and center hub will generate some vibratory loads due to blockage effects. For example, Fig. 12 shows the oscillatory loads in the axial (thrust) direction with the total thrust normalized by its

azimuth-averaged thrust. At a pitch angle of 20 deg, the peak-to-peak value reaches 12% of the total thrust, which is a significant vibratory load. The relative fluctuation decreases as blade pitch increases, which is similar to the phenomenon observed and explained in the discussion of the oscillating force in the rotating frame. One significant distinction between Fig. 11 and Fig. 12 is the frequency of the fluctuation in each blade rotation. In the fixed frame, a strong 6/rev thrust occurs because six blades are used.

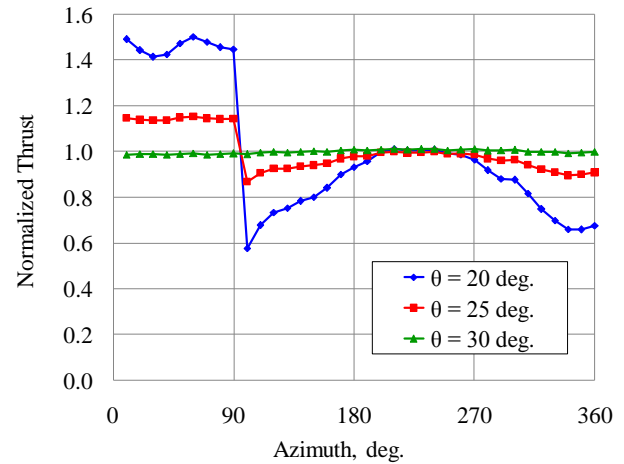


Figure 11: Normal force fluctuation at blade root

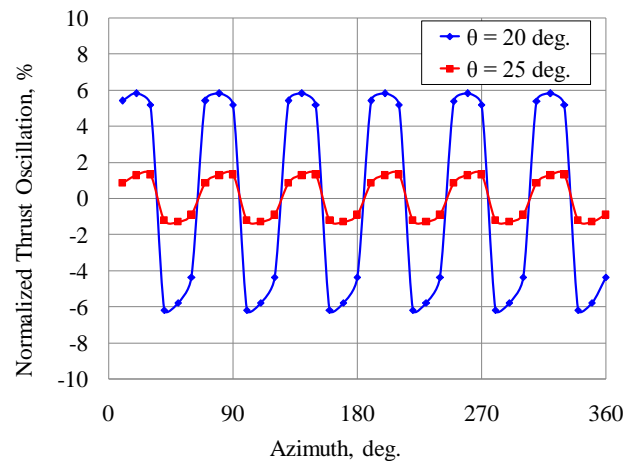


Figure 12: Hub oscillatory loads due to blockage

Due to the blockage in one quarter of the duct inlet, the total thrust is no longer acting on the centerline of the propulsor shaft. Figure 13 illustrates the thrust offsets in the yaw (side) direction in terms of the ratio of the yawing moment to averaged total thrust. Comparing with zero offset in the case of no blockage effects, there is a large oscillating offset existing in this case. A similar phenomenon was observed for the pitching moment, as shown by Fig. 14. Actually due to the blockage in a quarter of the duct inlet, vibratory loads are excited in all forces and moments. These vibratory loads must be considered in the design of the ducted propulsor system.

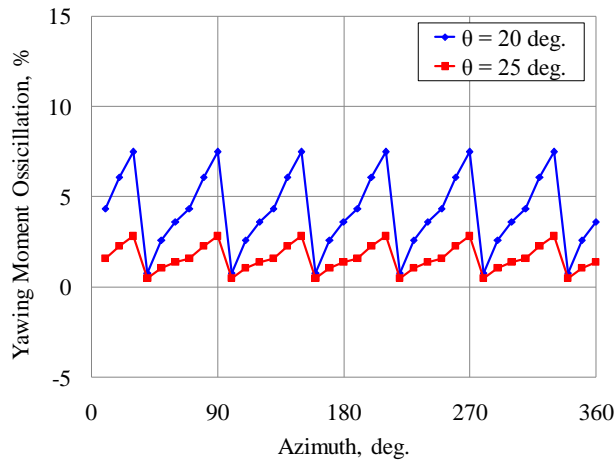


Figure 13: Vibratory yawing moment due to blockage

When discussing blockage effects, one note should be made on what reference airspeed should be used in the calculation of the efficiency of a ducted propulsor system tested in a wind tunnel. Conventionally, for an isolated propeller operating in an open air environment, the reference flow speed should be the undisturbed, uniform free stream speed in front of the ducted propulsor system. However, for a complete ducted propulsor system tested in a wind tunnel, there is typically some superstructure upstream of the duct inlet and a wave fence along side of the duct. The flow pattern can be very complicated, and therefore, it is hard to have a reference velocity that is fully compatible with the free stream velocity. The difference between the real flow the ducted propulsor system experienced in real time and the conventionally used reference flow speed in the open air can greatly affect the magnitudes of the efficiency calculated. Hence, caution needs to be taken when comparing wind tunnel results with theoretical values.

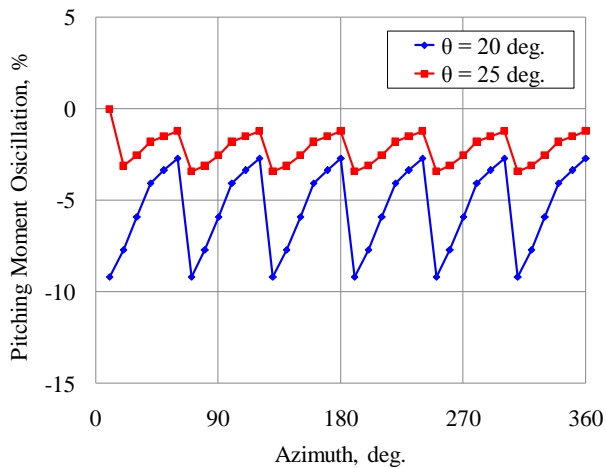


Figure 14: Vibratory pitching moment due to blockage

3.4 Sensitivity to other design parameters

Blade twist is an important design parameter that can be utilized to optimize the blade load distribution. Generally, it is desirable that the blade features a negative twist distribution along the span, decreasing the pitch angle

from the blade root to tip. Theoretically, the ideal twist for a blade operating in the static condition should be in a hyperbolic form, i.e., it is reversely proportional to blade span-wise station ($1/r$, r is radial station from the blade root). With an ideal twist, the blade could create a uniform inflow that must always correspond to the minimum induced power when the blade is operating in an axial flow environment, which is the case for a ducted aerodynamic propulsor. Unfortunately, the hyperbolic form of twist distribution is physically unrealizable as r approaches zero. However, because of the low velocity near the blade root, the blade pitch variation near the blade root has little effect. Therefore, a large negative twist instead of ideal twist is typically used. To evaluate the effect of blade twist on performance, the total nonlinear twist of the fan blade was changed from negative 40 degrees (baseline configuration) to negative 20 degrees. The results are shown by Fig. 15 for the bollard condition. It is clear that the propulsor with a negative 20 degree twist blade is approximately 7% less efficient than the baseline configuration at a fan rotational speed of 1,300 rpm.

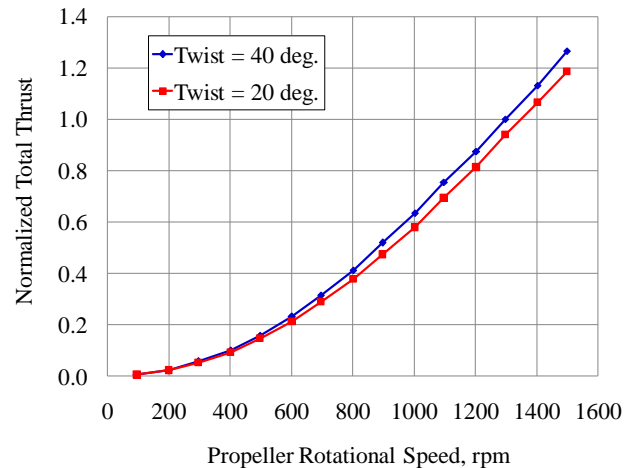


Figure 15: Effect of blade twist

Another important design parameter investigated is the blade tip clearance between the blade and shroud. Any gap that exists can cause air leakage and therefore, can reduce the efficiency of the blade. However, manufacturing the ducted propulsor with very small tip clearance is challenging. Three different blade tip clearances; no gap, 1.0%R and 3.0%R, were examined. Figure 16 shows the normalized power required at different thrust levels in the bollard condition. These analytical results indicate that for the baseline configuration propulsor efficiency is insensitive to blade tip clearance when the clearance is between one and three percent of propulsor radius. However, as the tip clearance approaches zero, propulsor efficiency can be quite sensitive to gap size. Therefore, in the ducted propulsor design, the clearance between blade tip and the surrounding duct should be kept as small as possible.

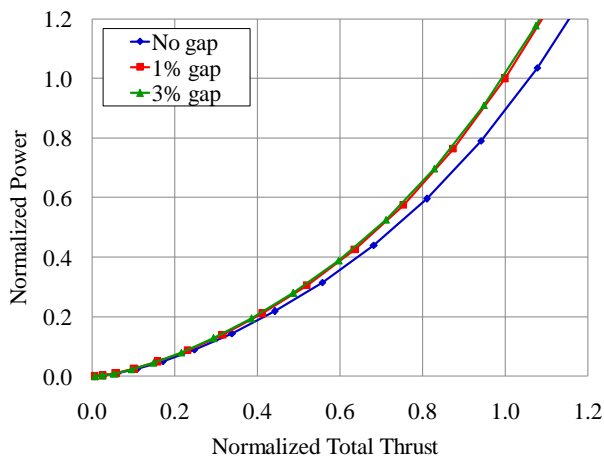


Figure 16: Blade tip clearance effects

Performance of three different propulsor locations within the duct has also been evaluated for a pitch setting of 30 deg and a fan rotational speed of 1,300 rpm in the bollard condition. For the baseline configuration, the propulsor is located within the duct at 0.20R from the duct inlet. Two other cases were evaluated; one with the propulsor moved towards the inlet of the duct (0.05R from the duct inlet) and another with the propulsor moved downstream (0.5R from the duct inlet). Results are shown in Fig. 17. It is interesting to note that moving the fan in either direction reduced the efficiency of this ducted propulsor system (approximately 3%). Further study is required to optimize the propulsor location within the duct.

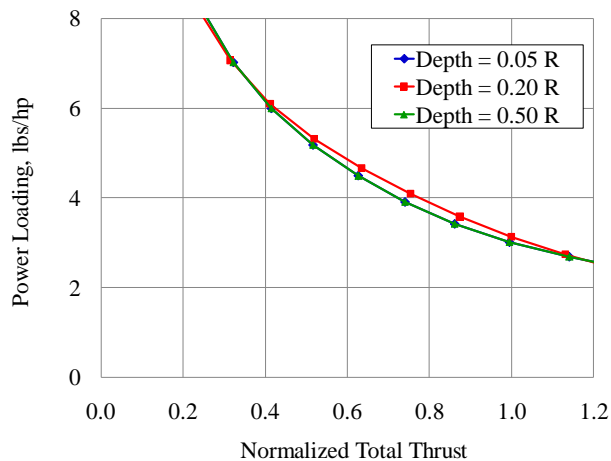


Figure 17: Effects of fan depth within duct on performance

4 SUMMARY AND CONCLUSIONS

A comprehensive analytical model of a generalized aerodynamic ducted propulsor system representative of those utilized for shipboard applications has been developed and validated with available experimental data. The model can be used accurately and efficiently to analyze the performance of a complete ducted aerodynamic propulsor system which consists of a shrouded duct, a fan and stators. The analytical model

utilizes a panel method approach to represent the duct, center hub and stators, and a blade element approach to represent the rotating blades. Mutual aerodynamic interactions between each aerodynamic component are included. In addition to the performance characteristics of the baseline configuration, the effects of aerodynamic compressibility on the propulsive efficiency were examined for both the baseline configuration and a configuration with advanced airfoils. A generalized approach for simulating the blockage effects from the superstructure upstream of the duct was also developed. In addition, the sensitivity of certain design parameters on performance was investigated. The following conclusions and recommendations are made based on the results of this study.

- (1) For the ducted propulsor system investigated, the duct can account for up to 40% of total thrust in the static bollard condition, which is very significant. Even though the duct contribution to the total thrust decreases gradually with increasing free stream speed, it still accounts for approximately 25% of the total thrust at a free stream velocity of 50 kts. A focused effort needs to be made to optimize the duct contribution to total thrust in the design of a ducted aerodynamic propulsor system for shipboard applications.
- (2) Aerodynamic compressibility effects have a significant impact on performance of ducted aerodynamic propulsors. The performance efficiency is reduced by more than 10% at moderate and high blade pitch angles for both NACA 0012 and RC airfoils when the blade tip Mach number is greater than 0.70 which is typical. Therefore, compressibility effects on performance need to be accounted for in the blade design process.
- (3) A preliminary investigation of propulsor inlet blockage effects indicates that significant vibratory loads are induced in both the fixed and rotating frames (i.e., hub and blade) when a quarter of the duct inlet is blocked. For shipboard applications of ducted aerodynamic propulsors where significant superstructures are present upstream of the propulsor, a thorough evaluation of blockage effects should be conducted, especially as it relates to significantly increased vibratory loads in the propulsor.
- (4) Propulsor efficiency is insensitive to blade tip clearance when the tip gap is between 1%R and 3%R. However, as the tip clearance approaches zero, propulsor efficiency can be quite sensitive

to gap size. Therefore, the blade tip clearance should be kept as small as possible.

- (5) A negative 40 degree twist distribution in the blade results in higher efficiency compared to the case when twist was negative 20 degrees. Further study is required to achieve an optimum twist distribution.
- (6) The relative propulsor location within the duct is an important design parameter which can affect the efficiency of the ducted propulsor system.

ACKNOWLEDGEMENT

The authors wish to thank Mr. Alan Schwartz of NSWCCD for developing computational codes and for constructive discussion of results.

REFERENCES

Advanced Rotorcraft Technology, (ART), Inc., "FLIGHTLAB Theory manual," March 2004.

Naipai P. Bi, Chengjian He, "Investigation of Fan-In-Disk Aerodynamics In Edgewise Flight", Proceedings of the American Helicopter Society 64th Annual Forum and Technology Display, Montreal, Canada, 2008.

Donald Black, Harry Waiauski, "Shrouded Propellers – A Comprehensive Performance Study", NACA 68-994.

Donald Black, Harry Waiauski: Hamilton Standard Shrouded Propeller Test Program, Method Development, Hamilton Standard report HSER 4348, Volume II – IV (test data); May, 1967.

Gene J. Bingham, Kevin W. Noonan, "Two-Dimensional Aerodynamic Characteristics of Three Rotorcraft Airfoils at mach Numbers From 0.35 to 0.90", NASA TP 2000, May 1982.

Scott Gowing, "Propeller Inflow Measurements on an Air Cushion landing Craft Vehicle (LCAC)", NSWCCD-50-TR-2003/029, 2003.

Chengjian He and Hong Xin, "An Unsteady Ducted Fan Model for Rotorcraft Flight Simulation", Proceedings of the American Helicopter Society 62th Annual Forum and Technology Display, Phoenix, Az, 2006.

De Piolenc F. Marc and G.E. Write, Ducted Fan Design, Millennial Year Edition Vol. 1, 2001.

W. Morgan and E. B. Caster, "Comparison of Theory and Experiment on Ducted Propellers", Prepared for the Seventh ONR Symposium on Naval Hydrodynamics, Rome, Italy, 1968

Rose Worobel and Aldo A. Peracchio: Hamilton Standard Shrouded Propeller Test Program, Hamilton Standard report HSER 4776, Volume I (Method Development); January, 1968.